Chinese Chemical Letters 35 (2024) 109195

Contents lists available at ScienceDirect

Chinese Chemical Letters

journal homepage: www.elsevier.com/locate/cclet

Alcohothermal synthesis of sulfidated zero-valent iron for enhanced Cr(VI) removal

Zhongsen Wang[1], Lijun Qiu[1], Yunhua Huang, Meng Zhang, Xi Cai, Fanyu Wang, Yang Lin, Yanbiao Shi, Xiao Liu*

Engineering Research Center of Photoenergy Utilization for Pollution Control and Carbon Reduction of Ministry of Education, College of Chemistry, Central China Normal University, Wuhan 430079, China

ARTICLE INFO

Article history:
Received 27 June 2023
Revised 21 September 2023
Accepted 11 October 2023
Available online 13 October 2023

Keywords:
Zero-valent iron
Sulfidation
Alcohothermal method
Cr(VI) removal

ABSTRACT

Sulfidation of zero-valent iron (ZVI) has attracted broad attention in recent years for improving the sequestration of contaminants from water. However, sulfidated ZVI (S-ZVI) is mostly synthesized in the aqueous phase, which usually causes the formation of a thick iron oxide layer on the ZVI surface and hinders the efficient electron transfer to the contaminants. In this study, an alcohothermal strategy was employed for S-ZVI synthesis by the one-step reaction of iron powder with elemental sulfur. It is found that ferrous sulfide (FeS) with high purity and fine crystallization was formed on the ZVI surface, which is extremely favorable for electron transfer. Cr(VI) removal experiments confirm that the rate constant of S-ZVI synthesized by the alcohothermal method was 267.1- and 5.4-fold higher than those of un-sulfidated ZVI and aqueous-phase synthesized S-ZVI, respectively. Systematic characterizations proved that Cr(VI) was reduced and co-precipitated on S-ZVI in the form of a Fe(III)/Cr(III)/Cr(VI) composite, suggesting its environmental benignancy.

Zero-valent iron (ZVI), with high reduction capacity and environmental benignancy, has attracted extensive research attention for the removal of various water contaminants, such as halogenated organics, dye, heavy metals, and metal complexes [1–5]. Whereas, during the manufacturing or usage process, ZVI is easy to be covered by the oxide layer [6,7], severely preventing electron transfer and leading to low reactivity or durability in contaminants removal. In order to improve the reaction performance of ZVI for various pollutants, multiple measures have been developed to eliminate the iron oxide shell of ZVI [8], such as pickling [9,10], ultrasound [11,12], reduction [13,14], and magnetization [15,16]. However, due to the poor selectivity of ZVI to pollutants and the preference for hydrogen production reaction with water, it is not satisfactory to achieve efficient pollutants removal in water. Therefore, how to modify the outer-layer structures and optimize the performance of ZVI, improving both the reactivity and electron selectivity, remains a challenge.

Recently, the method of sulfidation has been applied to enhance the removal performance of ZVI [17,18]. During the sulfidation, an iron sulfide minerals shell is often formed on the surface of sulfidated ZVI (S-ZVI), which is a good semiconductor to promote the electron transfer of ZVI core to the target pollutant compared with the iron oxide on the ZVI surface [19–21]. At the same time, iron sulfide minerals shell can inhibit the binding of active hydrogen (•H) and promote pollutants reduction by •H [22]. Therefore, the functionalization of ZVI with iron sulfide minerals is an effective strategy to elevate the activity and selectivity of ZVI in pollutant remediation.

Generally, S-ZVI is prepared in an aqueous phase with dithionite or sodium sulfide (Na_2S) as a sulfur source, which brings several disadvantages. For example, when using dithionite as a sulfur source, ZVI was inclined to be oxidized by dithionite, thus resulting in substantial reactivity loss for contamination removal [23]. When Na_2S was utilized, the solution tended to release harmful H_2S into the air [24,25]. Accordingly, it is necessary to develop a new and facile S-ZVI synthesis method to avoid reactivity loss and toxic by-production formation.

In this study, we proposed a novel method of sulfidation of ZVI with S powders by alcohothermal method and found that ferrous sulfide (FeS) with high purity and fine crystallization was formed on the surface of ZVI. Taking Cr(VI) as the targeted contaminant, it is confirmed that the electron selectivity and removal performance of S-ZVI synthesized by the alcohothermal method were much higher than those of un-sulfidated ZVI and aqueous-

* Corresponding author.
E-mail address: liuxiao71@ccnu.edu.cn (X. Liu).
[1] These authors contributed equally to this work.

https://doi.org/10.1016/j.cclet.2023.109195
1001-8417/

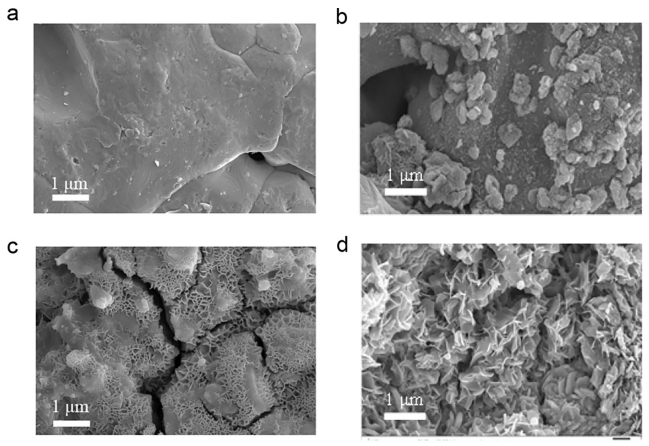

Fig. 1. SEM images of (a) ZVI, (b) S-ZVI$^{A}_{0.01}$, (c) S-ZVI$^{A}_{0.05}$ and (d) S-ZVI$^{A}_{0.10}$.

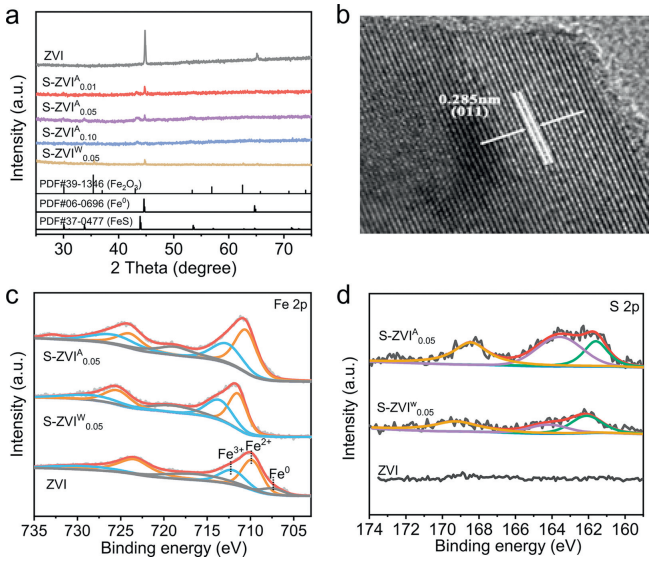

Fig. 2. (a) XRD patterns of samples. (b) HRTEM image of S-ZVI$^{A}_{0.05}$. XPS spectra of samples: (c) Fe 2p, (d) S 2p.

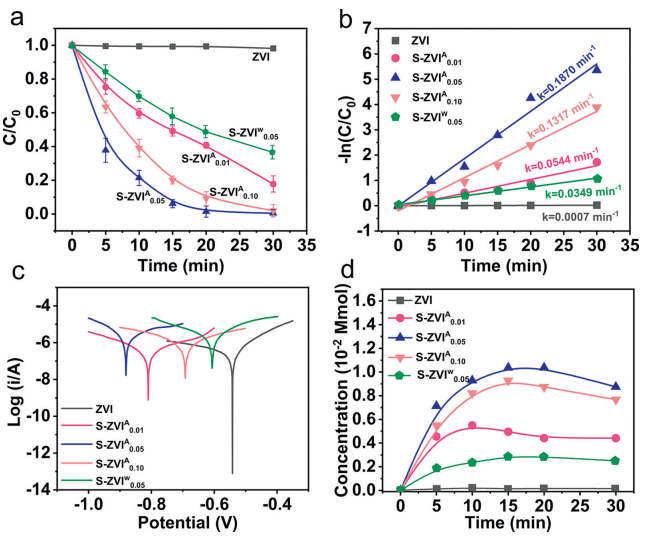

Fig. 3. (a) The Cr(VI) removal performance of samples. (b) *Pseudo*-first-order kinetics model for removal of Cr(VI). (c) Tafel scans in the absence of Cr(VI). (d) The release of Fe(II) from ZVI and S-ZVIs in the absence of Cr(VI).

phase synthesized S-ZVI. Systematic characterizations proved that Cr(VI) was reduced and co-precipitated on S-ZVI in the form of a Fe(III)/Cr(III)/Cr(VI) composite, suggesting its environmental benignancy.

The surface morphologies of pristine ZVI and S-ZVI^{A} were characterized by SEM. The untreated ZVI surface was found to be relatively smooth and dense (Fig. 1a). After the sulfidation under alcohothermal conditions, the surface roughness of ZVI increased significantly and some cracks with the width of several hundred nanometers appeared (Figs. 1b–d). More importantly, a large number of thin nanosheets were formed on the surface of ZVI, indicating the emergence of new phases during the alcohothermal treatment.

The XRD patterns (Fig. 2a) show two sharp peaks at 44.7° and 65.1°, corresponding to the (110) and (200) facets of Fe^0 [26], indicating that surface sulfidation did not alter the main structure of ZVI. At the same time, with the increase of the S/Fe mass ratio, some new characteristic peaks at about 43.4° appeared, verifying the formation of FeS [26,27]. TEM images (Fig. 2b and Fig. S1 in Supporting information) reveal the microstructure of the substances with a crystal plane spacing of 0.285 nm on the surface of S-ZVI^{A}, which is consistent with the (011) plane of FeS [28]. Combined with the XRD data, we can further identify the exist of FeS nanocrystals on the surface of S-ZVI^{A}. The surface compositions and chemical environments of these samples were obtained through XPS. From the Fe 2p XPS spectra (Fig. 2c), we can see that the Fe^0 feature peak at 707.4 eV on the surface of S-ZVI^{A} is missing, and the surface Fe(II) content at 710.0 eV is significantly increased [29]. The S 2p XPS spectra (Fig. 2d) confirms the presence of S species on the surface of S-ZVI^{A} [29]. Through water contact angle experiments, as shown in Fig. S2 (Supporting information), the contact angle of untreated ZVI is around 21°. After surface sulfidation, the contact angle of S-ZVI^{A} increases to around 33°, indicating that the material becomes more hydrophobic due to the formation of FeS layers.

Taking Cr(VI) as the target contaminant, the reactivity of S-ZVI samples was investigated at room temperature. As shown in Fig. 3a, Cr(VI) was completely removed by S-ZVI$^{A}_{0.05}$ within 30 min, while ZVI has almost no removal activity under the same reaction conditions. To quantify the influence of sulfidation on the reactivity of ZVI, the kinetic process of Cr(VI) removal was simulated by using the pseudo-first-order rate law (Fig. 3b). As the S/Fe mass ratio increased from 0 to 0.05, the rate constants (k) for Cr(VI) removal by S-ZVI^{A} gradually enhanced from 0.0007 min^{-1} to 0.1870 min^{-1}, increasing about 267 times. However, when the S/Fe mass ratio increased to 0.10, the rate constants decreased, which means the S/Fe mass ratio has its optimum. To exclude the effect of surface areas of S-ZVI^{A} on the Cr(VI) removal ability, their apparent rate constants were normalized by using specific surface areas (Table S1 in Supporting information). The lack of positive correlation between specific surface area and rate constant indicates that it is not the root cause of the improvement of Cr(VI) removal capacity.

As is well known, Cr(VI) can be reduced by direct electron supply from ZVI. Generally, the electrons transfer from ZVI to absorbed Cr(VI) is a rate-limiting step. Owing to its lower band gap (E_g = 0.2–1.0 eV) and strong reducibility, FeS has good electron conductivity and can act as the electron acceptor to promote Cr(VI) reduction [30]. To verify the influence of electron transfer on the removal performance of S-ZVI on Cr(VI), we measured the free corrosion potential of ZVI samples by Tafel polarization diagram (Fig. 3c). The free corrosion potentials of the ZVI samples are in the range of −0.88 V to −0.54 V, and their negative potentials follow a trend of S-ZVI$^{A}_{0.05}$ > S-ZVI$^{A}_{0.01}$ > S-ZVI$^{A}_{0.10}$ > S-ZVI$^{W}_{0.05}$ > ZVI. It is known that an electrode of a more negative free corrosion potential value possesses a higher electron transfer rate [31]. There-

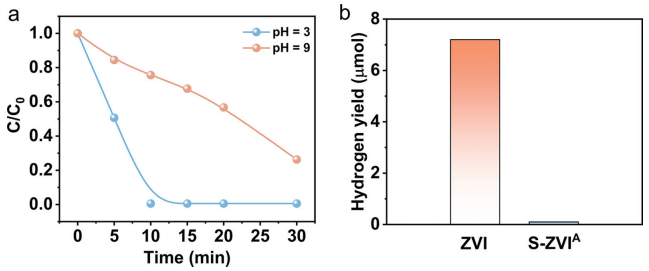

Fig. 4. (a) Effect of the initial pH for Cr(VI) removal. (b) Hydrogen yield with ZVI and S-ZVI^{A} during Cr(VI) removal process.

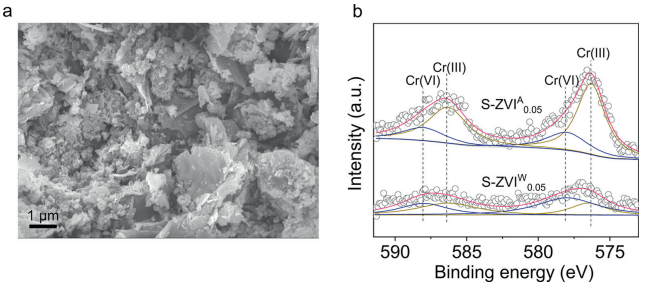

Fig. 5. (a) SEM image of S-ZVI^{W}. (b) Cr 2p XPS spectra of S-ZVI^{W} and S-ZVI^{A} samples after reactions.

fore, the electron transfer rate of the ZVI also follows the above trend. However, it is inconsistent with the normalized apparent constants (*k'*) for Cr(VI) removal by the S-ZVI, possibly due to some other reasons that influence the removal efficiency of Cr(VI). In addition to the direct reduction by electrons, Cr(VI) can also be rapidly reduced by Fe(II). We compared the concentration changes of Fe(II) release in an aqueous solution in the absence of Cr(VI) (Fig. 3d) and found that it fitted well with the Cr(VI) removal efficiency of S-ZVIs, indicating Fe(II) production is another key factor for Cr(VI) removal. Also, through comparing with the reported ZVI for Cr(VI) removal in literatures (Table S2 in Supporting information), the significantly advanced activity of the S-ZVI^{A} was demonstrated.

The removal process of Cr(VI) mainly consists of adsorption and reduction, where the adsorption process is caused by electrostatic interactions, hydrophobicity, and hydrogen bonding, which is largely influenced by pH [32–35]. As displayed in Fig. 4a, when pH = 3, Cr(VI) was completely removed within 10 min while the removal rate decreased by 24.4% at pH 9. Under acidic conditions, the surface of S-ZVI is positively charged, while Cr(VI) mainly exists in the form of $HCrO_4^{2-}/CrO_4^{2-}$, enhancing their electro-adsorption. At the same time, the corrosion rate of Fe is accelerated and the formation of Fe(II) can effectively reduce and remove Cr(VI). While under alkaline conditions, the surface of S-ZVI is negatively charged, which hinders the adsorption of Cr(VI).

The effects of dissolved oxygen on Cr(VI) removal were assessed and the results are shown in Fig. S3a (Supporting information). It is found that dissolved oxygen can promote Cr(VI) removal, which may be due to the promotion of ZVI corrosion and the release of Fe(II). This conjecture was then verified by the higher concentration of soluble Fe(II) under air than N_2 atmosphere (Fig. S3b in Supporting information). The electron utilization rate of ZVI in the Cr(VI) removal process counts a great deal because under acidic conditions, protons could compete with Cr(VI) to produce H_2 by reacting with electrons, resulting in hydrogen evolution corrosion of ZVI. Significantly, the H_2 yield decreased from 7.5 μmol to 0.1 μmol after the surface sulfurization of ZVI (Fig. 4b), possibly due to pendent protons of the FeS on the surface of S-ZVI^{A} hindered the evolution of H_2. This result indicates that surface sulfidation reduces the ineffective corrosion of ZVI and improves electron utilization for Cr(VI) removal.

According to the reported literature, the sulfidated S-ZVI^{W} was also synthesized in aqueous-phase conditions to compare the removal performance differences [36]. The phase structure and surface morphology of S-ZVI^{W} was characterized by XRD and SEM (Figs. 2a and 5a). We found both of the sulfidation methods could make ZVI surface rougher and the FeS phase was formed on the surface. However, under the same conditions, the removal percentage of Cr(VI) by S-ZVI^{W} was less than 65%, much lower than that of S-ZVI^{A} with the same S modification (Fig. 3a). From the Tafel scan in Fig. 3c, S-ZVI^{A} exhibited the more negative potentials than S-ZVI^{W} when S/Fe was 0.05, suggesting S-ZVI^{A} synthesized by alcohothermal method possesses a higher electron mobility. We also detected the Fe(II) dissolution for S-ZVI^{A} and S-ZVI^{W} in an aqueous solution and found that the Fe(II) concentration of S-ZVI^{A} was 3.5 times higher than that of S-ZVI^{W} (Fig. 3d). The difference in the content of Fe(II) on the surface is undoubtedly the main reason for the difference in activity between the two. Therefore, whether this difference will have an impact on the Cr(VI) reduction products, the Cr 2p XPS spectra of the two S-ZVI after reactions were tested, and the results are shown in the Fig. 5b. The broad peak of Cr $2p_{3/2}$ could be fitted to two peaks at 578.0 eV and 576.3 eV, which belongs to Cr(VI) and Cr(III) species, respectively [32,37]. The Cr(III)/total Cr ratios are 73% and 40% for S-ZVI^{A} and S-ZVI^{W} respectively, implying more Cr(VI) was reduced in the S-ZVI^{A} system. Also, it can be seen from Fig. S4 (Supporting information) that the contents of Fe(II) on the S-ZVI^{A} surface still accounts for 44% after reactions, while the proportion of S-ZVI^{W} is only 35%. We can conclude that the synthetic methods indeed have a vital impact on S-ZVI, affecting the corrosion of Fe^0 and the release of Fe(II) which have an important role in Cr(VI) removal.

Compared to the aqueous-phase synthetic method, alcohothermal synthesis can slow down the crystallization rate because of the weak polarity of the alcohol solvent, which is conducive to controlling the crystallization and morphology of solid products. From the environmental perspective, the use of alcohol and elemental S eliminates the risk of producing harmful H_2S. More importantly, benefiting from high temperature and a non-aqueous environment, the alcohothermal method is helpful to the formation of iron sulfide minerals with good crystallinity on the ZVI surface. Therefore, the alcohothermal method exhibits greater potential for the preparation of S-ZVI than the aqueous-phase synthetic method.

In summary, we prepared sulfidated ZVI by surface sulfidation in an alcohothermal environment. Choosing Cr(VI) as the model pollutant, we found that the rate constant of S-ZVI synthesized by the alcohothermal method was 267.1- and 5.4-fold higher than those of un-sulfidated ZVI and aqueous-phase synthesized S-ZVI, respectively. Combined with comprehensive characterization such as SEM, XRD, XPS, and Tafel polarization, it was found that different synthesis methods would lead to differences in the formation of iron sulfide and (hydro) oxides on the surface. Compared with the aqueous phase, the alcohol phase synthesis method could promote the corrosion of ZVI and avoid the formation of iron (hydro) oxides on the surface of ZVI. Cr(VI) was reduced and co-precipitated on S-ZVI^{A} in the form of a Fe(III)/Cr(III)/Cr(VI) composite, suggesting its environmental benignancy. This method is of great significance for the synthesis and modification of zero-valent iron to remove water pollutants.

Declaration of competing interest

The authors declare that they have no known competing financial interests or personal relationships that could have appeared to influence the work reported in this paper.

Acknowledgments

We acknowledge the National Key Research and Development Program of China (No. 2019YFC1806203) for financial support. We would like to thank Biao Wang from SCI-GO (www. sci-go.com) for the XPS analysis.

Supplementary materials

Supplementary material associated with this article can be found, in the online version, at doi:10.1016/j.cclet.2023.109195.

References

[1] Y. Hu, X. Peng, Z. Ai, et al., Environ. Sci. Technol. 53 (2019) 8333–8341.
[2] M. Liao, X. Wang, S. Cao, et al., ACS ES&T Water 1 (2021) 2109–2118.
[3] M. Li, Y. Mu, H. Shang, et al., Appl. Catal. B 263 (2020) 118364.
[4] L. Ling, C. Tang, W.X. Zhang, Environ. Sci. Technol. Lett. 5 (2018) 520–525.
[5] X. Wang, X. Pu, Y. Yuan, et al., Chin. Chem. Lett. 31 (2020) 2634–2640.
[6] M. Li, H. Shang, H. Li, et al., Angew. Chem. Int. Ed. 60 (2021) 17115–17122.
[7] S. Zou, Q. Chen, Y. Liu, et al., Chin. Chem. Lett. 32 (2021) 2066–2072.
[8] Y. Hu, G. Zhan, X. Peng, et al., Chem. Eng. J. 389 (2020) 124414.
[9] S.C. Popat, K. Zhao, M.A. Deshusses, Chem. Eng. J. 183 (2012) 98–103.
[10] S.L. Doty, J.L. Freeman, C.M. Cohu, et al., Environ. Sci. Technol. 51 (2017) 10050–10058.
[11] S. Lee, J. Hazard. Mater. 145 (2007) 17–22.
[12] Y. Quan, H. Wu, C. Guo, et al., Bioresour. Technol. 259 (2018) 365–372.
[13] S. Bae, S. Gim, H. Kim, et al., Appl. Catal. B 182 (2016) 541–549.
[14] K.J. Lampron, P.C. Chiu, D.K. Cha, Water Res. 35 (2001) 3077–3084.
[15] S.C. Popat, M.A. Deshusses, Environ. Sci. Technol. 43 (2009) 7856–7861.
[16] L. Rajic, N. Fallahpour, S. Yuan, et al., Water Res. 67 (2014) 267–275.
[17] S. Cai, B. Chen, X. Qiu, et al., Environ. Sci. Technol. 55 (2021) 645–654.
[18] L. Gong, J. Chen, Y. Hu, et al., Environ. Sci. Technol. 57 (2023) 9811–9821.
[19] J. Li, X. Zhang, M. Liu, et al., Environ. Sci. Technol. 52 (2018) 2988–2997.
[20] S.R.C. Rajajayavel, S. Ghoshal, Water Res. 78 (2015) 144–153.
[21] S. Huang, C. Xu, Q. Shao, et al., Chem. Eng. J. 338 (2018) 539–547.
[22] J. Hou, A. Wang, L. Miao, et al., Sci. Total Environ. 829 (2022) 154304.
[23] Y. Xie, D.M. Cwiertny, Environ. Sci. Technol. 44 (2010) 8649–8655.
[24] Y. Gu, B. Wang, F. He, et al., Environ. Sci. Technol. 51 (2017) 12653–12662.
[25] Y. Gu, L. Gong, J. Qi, et al., Water Res. 159 (2019) 233–241.
[26] C. Xu, C. Yang, X. Liu, et al., J. Hazard. Mater. 417 (2021) 126019.
[27] F. He, Z. Li, S. Shi, et al., Environ. Sci. Technol. 52 (2018) 8627–8637.
[28] K. Chen, K. Cao, C. Xing, et al., J. Alloys Compd. 688 (2016) 946–952.
[29] N. Liu, Y. Gong, X. Peng, et al., J. Hazard. Mater. 432 (2022) 128683.
[30] M.A. Irham, F. Muttaqien, S.Z. Bisri, et al., J. Phys. Chem. Lett. 12 (2021) 10777–10782.
[31] D. Liu, X. Peng, B. Wu, et al., J. Am. Chem. Soc. 137 (2015) 9772–9775.
[32] X. Guan, H. Yang, Y. Sun, et al., Chemosphere 228 (2019) 370–376.
[33] L. Jia, X. Tan, Y. Li, et al., Chin. Chem. Lett. 33 (2022) 3053–3060.
[34] H. Zhang, D.L. Liu, L.L. Zeng, et al., Chin. Chem. Lett. 24 (2013) 341–343.
[35] X.H. Yi, Y. Gao, C.C. Wang, et al., Chin. Chem. Lett. 34 (2023) 108029.
[36] Q. Shao, C. Xu, Y. Wang, et al., Water Res. 135 (2018) 322–330.
[37] B. Xie, C. Shan, Z. Xu, et al., Chem. Eng. J. 308 (2017) 791–797.